Journal of Colloid and Interface Science 587 (2021) 14–23

Contents lists available at ScienceDirect

Journal of Colloid and Interface Science

journal homepage: www.elsevier.com/locate/jcis

Regular Article

The role of microparticles on the shape and surface tension of static bubbles

H. Wang *, P.R. Brito-Parada *

Department of Earth Science and Engineering, Imperial College London, London SW7 2AZ, UK

GRAPHICAL ABSTRACT

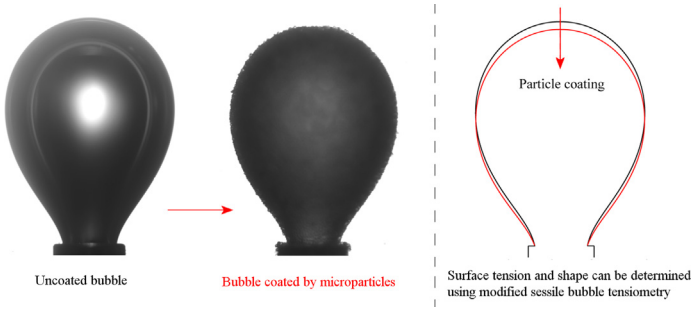

ARTICLE INFO

Article history:
Received 10 June 2020
Revised 23 November 2020
Accepted 24 November 2020
Available online 30 November 2020

Keywords:
Surface tension
Particle-laden bubble
Sessile bubble method
Bubble shape
Particle-bubble interaction force

ABSTRACT

Hypothesis: Surface tension is a critical parameter in bubbles and foams, yet it is difficult to assess when microparticles are attached at the interface. By considering the interaction force between an air–liquid interface and microparticles, modified equations for sessile bubble tensiometry can be derived to determine the surface tension and shape of static microparticle-laden bubbles.
Experiments: A modified sessile bubble method, in which the forces between microparticles and the air–liquid interface are considered, was developed and used to analyse the surface tension of bubbles fully coated by a monolayer of silica microparticles of different sizes. The results are compared to those obtained using classical sessile bubble tensiometry. The new method is also used to investigate the contours of particle-laden bubbles of varying particle radius and contact angle.
Findings: While the classical sessile bubble method overestimates the surface tension, results obtained using the modified sessile bubble method show that the surface tension of static microparticle-laden bubbles remains the same as that of uncoated bubbles, with no dependency on the particle size. The discrepancy is due to the fact that microparticles attached to the air–liquid interface deform a bubble in a similar way that changes in surface tension do for uncoated bubbles.

1. Introduction

Interfacial tension plays a key role in products [1,2] and processes [3,4] where the capillary length scale is dominant. It originates from unbalanced intermolecular forces near a fluid–fluid interface and represents the surface energy per unit interfacial area [5,6]. Interfaces have a tendency to minimise the surface energy by spontaneously exhibiting a minimum surface area. Interfacial tension not only determines the shape of drops or bubbles [7–9] but also affects the interface dynamics during pinch-off [10], oscillation [11,12] and coalescence [13] of bubbles or drops. An accurate

* Corresponding authors.
E-mail addresses: hao.wang16@imperial.ac.uk (H. Wang), p.brito-parada@imperial.ac.uk (P.R. Brito-Parada).

https://doi.org/10.1016/j.jcis.2020.11.094
0021-9797/

measurement of the interfacial tension of bubbles or drops is thus of fundamental importance in understanding systems such as foams and emulsions.

Particle-laden interfaces are at the core of froth flotation, the most important separation technique in mineral processing and also key in paper deinking, plastic recycling, and water treatment [14]. The stability of flotation froths, i.e. particle-laden foams, is linked to the recovery of particles and significantly affected by particle size [15,16]. In addition to froth flotation, particle-laden interfaces continue to find applications in emerging technologies such as the preparation of bijels [17], drug delivery [18] and interfacial catalysis [19].

The effect of particles at fluid–fluid interfaces on the interfacial tension has received increasing attention [20]. Although silica nanoparticles have been shown to be foam and emulsion stabilisers [1,2,21], the link between the stability of particle-laden foams or emulsions and the interfacial tension remains relatively less explored. This is partly due to the challenge in determining the interfacial tension of particle-laden interfaces.

While surfactants reduce the interfacial tension by weakening molecular interactions near the interface [22,23], nanoparticles reduce it by generating surface pressure as a result of interparticle interactions [24–27]. The surface pressure generated by nanoparticles acts in the opposite direction to the surface tension [20]. The size and contact angle of nanoparticles, as well as their packing structure at the interface, in a surfactant free system have been shown to affect surface tension [28]. The contact angle of nanoparticles influences the capillary attraction between the particles, which determines the packing structure of the particles at the interface [29]. The effective nanoparticle size, i.e. the distance between the centroid of two particles, has also been found to affect the interfacial tension, since varying the surface coverage of the particles at the interface leads to changes in the interparticle potential [24].

For interfaces coated by nanoparticles, the fact that nanoparticles adsorb or desorb from the interface on a time scale of normally minutes or even hours, makes the maximum bubble pressure method unsuitable for measuring the interfacial tension of nanoparticle-laden interfaces. Sessile bubble and pendant drop tensionmetry, however, have been proven to be reliable ways to measure the interfacial tension of these systems, even when the interface experiences deformation such as contraction or expansion [24]. The sessile bubble and pendant drop methods involve determining the interfacial tension from fitting the bubble or drop profile to Laplace's equation; differential equations derived from Laplace's equation are numerically solved and the interfacial tension is obtained from the best fitting to the bubble or drop contour. Sessile bubble and pendant drop tensiometry have been shown to be accurate methods to measure the interfacial tension over long time scales up to hours, while this is in the order of minutes for the maximum bubble pressure method and below milliseconds for the oscillating jet method [7].

For air–liquid interfaces coated by microparticles, the measurement of surface tension using the maximum bubble pressure method requires the attachment of the particles to the interface during the measurement, which can be achieved via mechanical stirring [30]. Once the stirring stops, microparticles normally settle from the suspension, unless they attached to the air–liquid interface and formed a close-packed structure at the interface [3,4,31]. This is dramatically different to a system with nanoparticles, for which adsorption occurs [32] without the need for stirring. The turbulence flow near the air–liquid interface as a result of the stirring might take the air–liquid interface out of equilibrium, which might affect the pressure inside the bubble and thus affect the surface tension measurement. The requirement of the stirring in the maximum bubble pressure method thus limits its application in determining the surface tension of microparticle-laden interfaces. Measurements based on the sessile bubble method, on the other hand, can be carried out when the stirring stops and a desired particle attachment to the interface has been achieved, in principle making the sessile bubble method a good alternative to measure the surface tension of microparticle-laden interfaces. However, two issues arise when using the sessile bubble method to determine the surface tension of microparticle-laden interfaces. Firstly, due to the relatively large size of microparticles, the particles attached to the air–liquid interface need to be removed when determining the bubble contour using image analysis. Secondly, microparticle gravity cannot be ignored, as is the case for nanoparticles. The force between the particles and the interfaces therefore needs to be considered in the equations for the classical sessile bubble method because this force might change the bubble shape and influence the surface tension measurement.

This work develops a fundamental understanding of the role of microparticles on the shape and surface tension of bubbles using a modified sessile bubble method. In this modified method, the equations from classical sessile bubble tensiometry were modified and then solved numerically using the fourth-order Runge–Kutta method [33]. The contour of the air–liquid interface, to which the modified equations were fitted, was obtained using a MATLAB image analysis routine. The surface tension of microparticle-laden bubbles was then determined from the best fit. The modified sessile bubble method developed allowed the investigation of the contour of particle-laden bubbles with different particle sizes and contact angles.

2. Theoretical analysis

2.1. The shape of uncoated bubbles

The shape of a static uncoated bubble can be described by the Young–Laplace equation, which relates the pressure difference across the air–liquid interface to the surface tension and the radius of curvature of the interface [7,31,34]. The surface tension minimises the surface area of the bubble while buoyancy forces resist the surface area minimization trend by stretching the bubble along the vertical axis. The importance of the gravitational force compared to the surface tension is described by the Bond number, $Bo = \Delta\rho g R_0^2/\gamma$, where $\Delta\rho$ is the density difference between the liquid and the air, g is the gravitational acceleration, R_0 is the radius of the bubble and γ is the surface tension of the air–liquid interface [7]. Assuming a constant air pressure P_g inside the bubble, the pressure difference across the air–liquid interface is then written as $(P_l - P_g)$, which equals $\gamma(1/R1 + 1/R2)$, where $1/R1$ and $1/R2$ are the principal radii of curvature of the interface (as illustrated in Fig. 1) and and P_l is the hydrostatic pressure of the liquid and can be determined by Pascal's law. The origin of the coordinate system was defined at the bubble apex (highest point of the bubble). x and z were defined as the horizontal and vertical axes, respectively, while s was defined as the arc length from the origin, as shown in Fig. 1. The hydrostatic pressure difference of the liquid between the origin and a position with a coordinate (x, z, s) is determined as $\Delta\rho gz$. The principal radii of curvature at the origin of the coordinate are: $R1 = R2 = R$. Eqs. (1)–(3) are three differential equations based on Young–Laplace equation and geometrical considerations. Eq. (4) is the boundary condition for Eqs. (1)–(3). The surface tension is determined by solving Eqs. (1)–(4) numerically using the fourth-order Runge–Kutta method and fitting to the contour of the bubble.

$$\frac{d\phi}{ds} = -\frac{sin\phi}{x} + \frac{2}{R} - \frac{\Delta\rho gz}{\gamma} \tag{1}$$

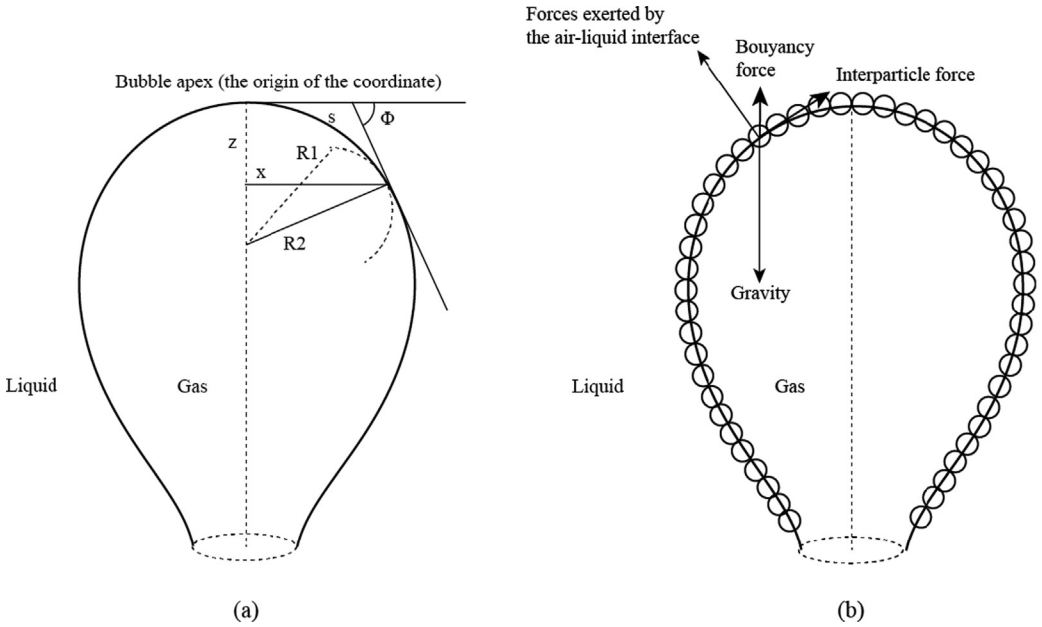

Fig. 1. (a) A schematic of a bubble illustrating the parameters used in the sessile bubble method; (b) a schematic of the force balance on a particle at the air–liquid interface, where small circles represent particles (not to scale).

$$\frac{dx}{ds} = cos\phi \tag{2}$$

$$\frac{dz}{ds} = sin\phi \tag{3}$$

$$0 = x(s=0) = z(s=0) = \phi(s=0) \tag{4}$$

2.2. The shape of particle-laden bubbles

For microparticle-laden bubbles, particles attached to the air–liquid have been observed to have a tendency to adopt a close-packing structure at the interface [3,4,31]. Contrary to nanoparticle systems, Brownian motion does not play a role in static microparticle-laden interfaces, in which particles remain still at the interface. The interparticle forces are thus in a balanced state, in contrast to what has been observed for microparticles at deforming interfaces such as during bubble coalescence [3] and pinch-off [4], where interparticle interactions lead to the generation of surface pressure and change the apparent surface tension of the air–liquid interface.

The forces exerted on the air–liquid interface by microparticles can deform the bubble compared to the shape of an uncoated bubble. If the interaction force between particles and the interface is not considered, the surface tension of microparticle-laden bubbles obtained from the best fit of the above four differential equations (Eqs. (1)–(4)) to the bubble coutour is expected to be higher than that of the uncoated bubbles. A modified sessile bubble method is presented here in which the mass of particles per unit area at the air–liquid interface is calculated to be $\frac{4\times10^{-6}}{3}P_{pk}\rho_p R_p$, where P_{pk} is the packing efficiency of the particles at the interface, defined as the ratio of the air–liquid area occupied by particles over the total area (i.e. the area occupied by particles and the voids between them) in a cell of fixed geometry. ρ_p is the density of the particles and R_p is the radius of the particles. The mass of particles at the bubble surface per unit area is determined from simple geometrical considerations. As the particle size is known beforehand, considering the fact that particles are closely packed at the interface, the number of particles per unit area can be determined first by $P_{pk}/(\pi R_p^2)$, from which the mass of particles per unit area is obtained by multiplying the particle number by the mass per particle $\frac{4}{3}\pi\rho_p R_p^3$. The mass of particles per unit area in contact with the liquid is $\frac{10^{-6}}{3}P_{pk}\rho_p R_p(2-cos\theta)(1+cos\theta)^2$ and the mass of particles per unit area in contact with the gas is $\frac{10^{-6}}{3}P_{pk}\rho_p R_p(2+cos\theta)(1-cos\theta)^2$, where θ is the contact angle of the particles in the liquid, as illustrated in Fig. 2. Considering the buoyancy force exerted on the particles in contact with the liquid, the force that particles exert on the interface per unit area P_{surf} can be calculated by Eq. (5) based on static force balance, as shown in Fig. 1b, where ρ_l is the density of the liquid. A term to consider the interaction force between the particles and the interface can be added to Eq. (1), which leads to Eq. (6). The new differential equation can thus be solved numerically to obtain the surface tension of bubbles coated by microparticles. The contour of microparticle-laden bubbles of different particle properties can also be investigated using our modified sessile bubble method.

$$P_{surf} = \frac{10^{-6}}{3}P_{pk}R_p g(1-cos\phi)[(2-cos\theta)(1+cos\theta)^2(\rho_p-\rho_l) + (2+cos\theta)(1-cos\theta)^2\rho_p] \tag{5}$$

$$\frac{d\phi}{ds} = -\frac{sin\phi}{x} + \frac{2}{R} - \frac{\Delta\rho g z}{\gamma} + \frac{P_{surf}}{\gamma} \tag{6}$$

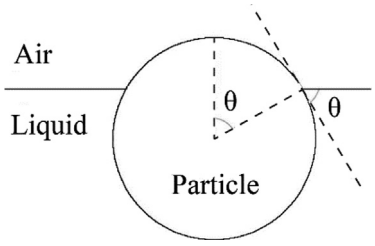

Fig. 2. Schematic of the particle at the air–liquid interface, where the contact angle of the particles in liquid, θ, is indicated.

3. Experimental

3.1. Particle size distribution

Soda lime glass bead particles were obtained from Sigmund Lindner GmbH and were used as received. The particles are naturally hydrophilic and acquire negative charge in water. Three particle size classes were used. The size distribution of the particle samples was determined using a Malvern Mastersizer 3000. Particle size distributions and cumulative volume fraction for three particle size classes can be found in Fig. S1 in the Supplementary Material. The particle size classes exhibited volume mean diameters D(4, 3) of 27.5 μm, 45.5 μm, 57.1 μm. The volume mean diameter D(4, 3) was used as the representative size of the particle size distribution as the mass of particles can be calculated more accurately in the modified sessile bubble method.

3.2. Attachment of microparticles to a static bubble

250 mL tetradecyltrimethylammonium bromide (TTAB) solution was prepared at a concentration of 10^{-6} M in a transparent perspex cell (50 mm × 50 mm × 125 mm). Deionised (DI) water with a resistivity above 15 MΩ cm was used to prepare the TTAB solution. Two grams of the soda lime particles were added to the TTAB solution and mixed for 10 min using a magnetic stirrer. Once the stirring stopped, particles started to settle to the bottom of the perspex cell. An individual bubble was produced from a nozzle submerged in the solution by pumping air via the micro-syringe pump (World Precision Instrument) after the particles settle completely. The outside diameter of the nozzle is 1.27 mm. The nozzle was adjusted based on image analysis to ensure it was vertically aligned. The size of the bubble was controlled by adjusting air injection using the micro-syringe pump. The micro-syringe pump stopped when the bubble radius reached approximately 1.6 mm, corresponding to a bubble volume of 17.2 mm^3, at which point the bubble was close to pinch-off. In order to achieve particle attachment to the bubble, particles were suspended via stirring. The low TTAB concentration guaranteed a negligible change in the surface tension (see Fig. S2 in the Supplementary Material) while still enhancing particle attachment at the air–liquid interface [4].

As reported by Berry et al. [7], the volume of the fluid affects the accuracy in pendant drop experiments and a large error might occur if the fluid volume is small. Note that bubbles prepared in our work are close to pinch-off and the size of the bubbles is large enough to give the most accurate and precise measurement using the sessile bubble method. Fig. 3a shows an uncoated bubble and Fig. 3b, c and d show bubbles fully coated by particles of three different size classes: 27.5 μm, 45.5 μm and 57.1 μm. A close-up view of the particle-laden bubble shows that a monolayer of particles exhibiting a hexagonal packing was present at the air–liquid interface, as illustrated in Fig. 3e. Particles were mostly closely packed at the interface, although some voids arise due to the size polydispersity of the particles. The contact angle of particles in the TTAB solution was determined by comparing the length of the three phase contact line and particle diameter, similar to the technique presented in [35], as illustrated in S3 in the Supplementary Material. The contact angle (θ) of the particles in this study was determined to be 38°, slightly higher than the value for silica particles in Cetyltrimethylammonium bromide (CTAB) solution reported by Ata [36,37].

3.3. Image analysis

Images were taken using a Canon EOS 600D camera with a resolution of 1.2 μm/pixel and a size of 6000 pixel by 4000 pixel. The original image, as shown in Fig. 4a, was processed using a MATLAB image processing routine to obtain binary images b and c in Fig. 4), before extracting bubble edge points for analysis. As illustrated in image c, the bubble surface was smoothed by removing noise in image b. Note that particles in contact with liquid (indicated as a grey region in Fig. 4d and e) should be removed from the image to obtain the position of the air–liquid interface, which was achieved via morphological erosion of the bubble image in Fig. 4c. The particles at the bubble surface in the input image (Fig. 4c) were eroded away after applying a disk-shaped structuring element, resulting in the bubble image without particles, as illustrated in the black region in Fig. 4d. It is relevant to note that the radius of the structuring disk was smaller than the particle diameter since the size of particles in contact with the liquid was smaller than their diameter. The radius of the structuring disk for particle-laden bubbles with D(4,3) of 27.5 μm, 45.5 μm and 57.1 μm can be calculated as a function of contact angle $\theta, \frac{D(4,3)}{2}(1+cos\theta)$, and was found to be 24.6 μm, 40.7 μm, 51.0 μm, respectively.

4. Results and discussion

4.1. The surface tension of particle-laden bubbles

4.1.1. Surface tension determined using the classical sessile bubble method

To validate our MATLAB routine to solve the differential equations in the classical sessile bubble method and find the best parameters to fit the bubble contour, the surface tension value of uncoated bubbles determined using our MATLAB routine was compared with that from the maximum bubble pressure method. The results determined using the maximum bubble pressure method can be found in Fig. S2 in the Supplementary Material. The fitting obtained for the uncoated bubble using the classical sessile bubble method was displayed in Fig. 5. The solid line in Fig. 5a represents the contour of an uncoated bubble obtained from image analysis

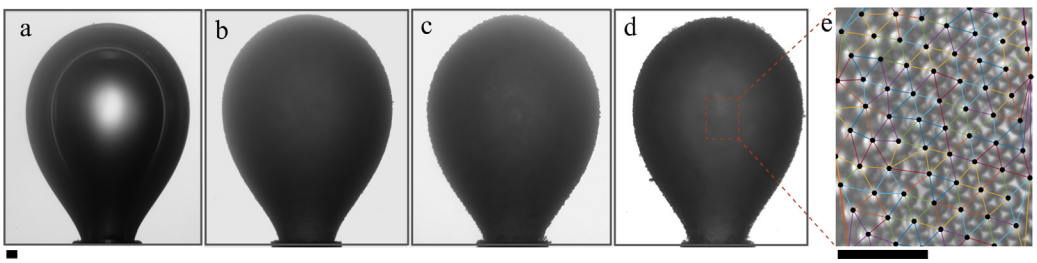

Fig. 3. A static uncoated bubble (a) and bubbles coated by particles of three different size classes: 27.5 μm (b), 45.5 μm (c) and 57.1 μm (d). The close-packed nature of particles at the air–liquid interface is also shown (e). Note that the central region of the bubble appears to be brighter due to the intensity of the LED light (this can be seen more clearly for the uncoated bubble in (a). Scale bars represent 0.20 mm.

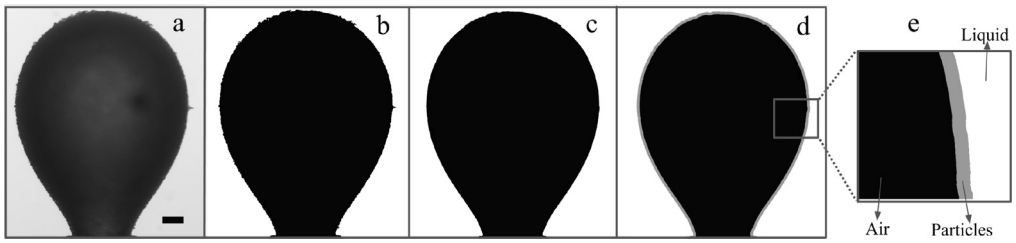

Fig. 4. Image processing procedure for obtaining the binary images for the modified sessile bubble method fitting: (a) Original image, (b) Thresholding, (c) Noise removal, (d) Removal of particles in contact with water (the grey region). (e) A close-up view of the particle-laden bubble surface. The scale bar is 0.35 mm.

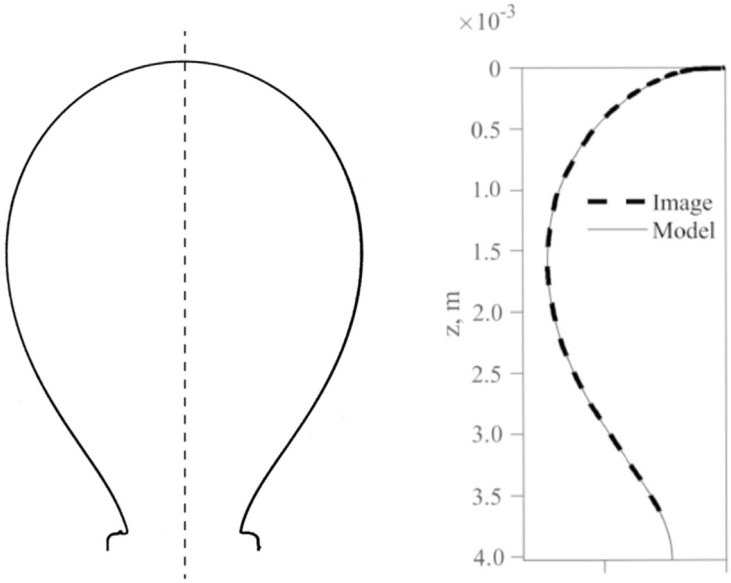

Fig. 5. (a) The contour of an uncoated bubble obtained from image analysis. The dashed line is the line of symmetry. (b) Image showing the contour of the left half of an uncoated bubble (dashed line) and the fitting to the bubble contour (solid line) using sessile bubble tensiometry.

while the dashed line indicates symmetry about the vertical axis. Fig. 5b shows the contour of the left half of the uncoated bubble (dashed line), which was used for the fitting to the sessile bubble model (Eqs. (1)–(4)). During the fitting, the radius of curvature at the bubble apex R and the surface tension were used as adjusting parameters. It can be seen from Fig. 5b that the solid line, which is the best fitting to the sessile bubble model, closely agrees with the bubble contour. The average surface tension, determined by the average of the three repeats of the surface tension obtained from the best fit, was 72.10 mN/m with a standard deviation of 0.26 mN/m, which agrees well with the results from the maximum bubble pressure method (see Fig. S2 in the Supplementary Material). The radius of curvature at the bubble apex R was 1.41 mm, smaller than the bubble radius R_0 (1.59 mm). The Bond number was calculated to be 0.34.

After validating our MATLAB routine for uncoated bubbles, the surface tension value of particle-laden bubbles was determined using the classical sessile bubble method, i.e. directly using Eqs. (1)–(4) to fit the edges of the original images, as illustrated in Fig. 6. Table 1 shows the fitting results of the radius of curvature at the bubble apex R, the capillary length and the surface tension γ of the particle-laden bubbles for three particle size classes determined using the classical sessile bubble method. For each particle-laden bubble case, three repeats were conducted. It was found that the value of the surface tension obtained using the classical sessile bubble method was higher than the real surface tension of the uncoated bubbles, i.e. 72.10 mN/m, for all particle-laden cases. A higher radius of curvature at the bubble apex and Bond number were also observed for particle-laden bubbles compared to the uncoated bubbles.

4.1.2. Surface tension determined by a modified sessile bubble method

In the modified sessile bubble method, Eqs. (2)–(6) were solved numerically to determine the surface tension of particle-laden bubbles following the same procedure as that for solving Eqs. (1)–(4). Fig. 7 shows the modified sessile bubble model fittings to the bubble contour for bubbles coated by three particle size classes, i.e. 27.5 μm, 45.5 μm and 57.1 μm. Thick black lines in Fig. 7 are the bubble edges directly obtained after thresholding and removing noise on the original particle-laden bubble images. Red lines show the air–liquid interface obtained by removing particles in contact with water on the edges of particle-laden bubbles. Contrary to the result from the classical sessile bubble method, the result determined from the modified sessile bubble method correctly shows that the surface tension of particle-laden bubbles remains the same as that of the uncoated bubbles, with no dependency on the particle size classes. Compared to our modified sessile bubble method, the classical method overestimated the surface tension of particle-laden bubble since the interaction force between particles and the air–liquid interface was not considered and the particles in contact with water were not removed from the original images in the classical method. It is relevant to note that, as shown in Table 2, only removing the particles while using the classical sessile bubble method equations does not contribute significantly to reducing the error in the calculation of surface tension; applying the modified method equations, on the other hand,

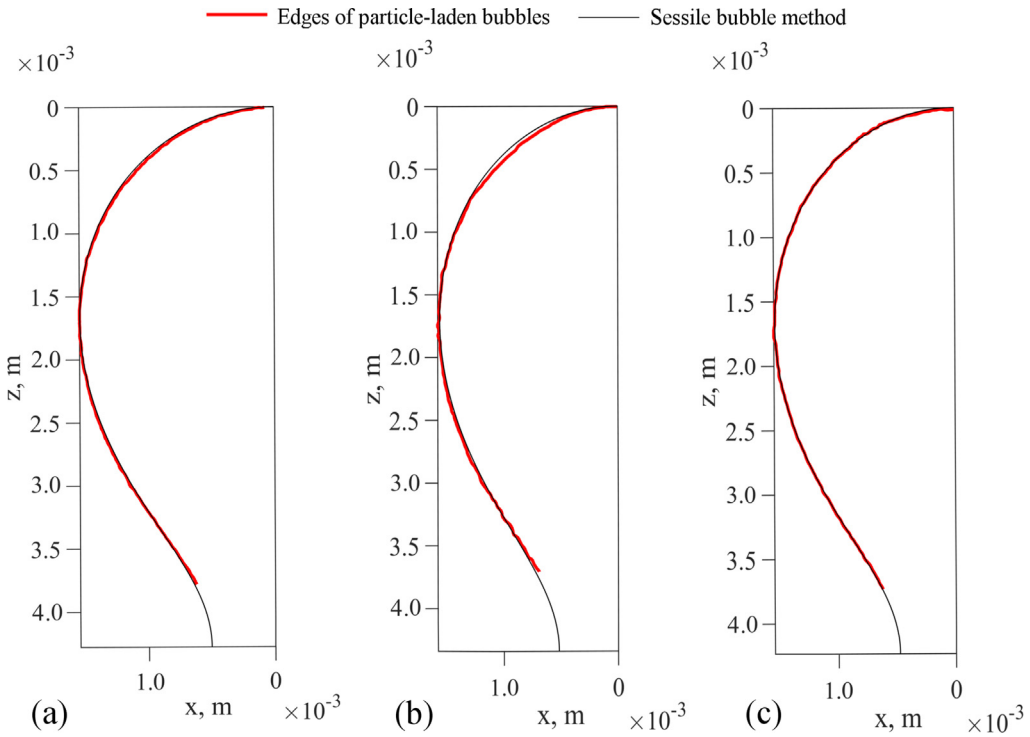

Fig. 6. Fittings obtained for particle-laden bubbles using the classical sessile bubble method. The particle size classes of the particle-laden bubbles are defined by their D(4,3): 27.5 μm (a), 45.5 μm (b) and 57.1 μm (c). Black lines show the fittings to the left half of the bubble contour obtained using the classical sessile bubble method (Eqs. (1)–(4)). Red lines are the edges of the particle-laden bubbles. Note that at this stage the particles were not removed from the particle-laden bubbles during. image analysis. (For interpretation of the references to colour in this figure legend, the reader is referred to the web version of this article.)

Table 1
Surface tension obtained directly from the classical sessile bubble method, i.e. using Eqs. (1)–(4) to fit the red lines in Fig. 6.

Particle size μm	The radius of curvature at the bubble apex mm	Capillary length mm	Surface tension mN/m	Bond number
[1.5ex] 27.5	1.46	2.79	76.14	0.37
	1.45	2.77	75.48	0.36
	1.46	2.80	76.64	0.37
45.5	1.48	2.79	76.32	0.38
	1.48	2.83	78.83	0.38
	1.48	2.83	78.66	0.38
57.1	1.47	2.81	77.34	0.37
	1.45	2.78	75.91	0.36
	1.43	2.79	76.36	0.35

leads to a significant reduction in the error, which is further minimised by also removing the particles.

To understand the reason why microparticles of silica do not change the surface tension of the static bubble, the effect of nanoparticles on the interfacial tension needs to be discussed and then compared to that of the microparticles. It is relevant to note that the focus here is on the effect of particles only, not on the effect of surfactants. For a discussion on the transfer of surfactant molecules between the particle surface and the bubble surface, i.e. the synergistic effect of the particles and the surfactant, the reader is referred to the work by Ata [36], Bournival et al. [38]. Nanoparticles have been proved to be able to stabilise foams and emulsions [1,2,21]. In particular, foams stabilised by silica nanoparticles have been found to last for hours [1]. The mechanism behind the increase in foam stability was related to the decrease in the surface tension of the nanoparticle-laden interfaces [39]. Garbin et al. [25] demonstrated experimentally and numerically that nanoparticles adsorbed at the deforming fluid–fluid interface decrease the interfacial tension by generating a two-dimensional pressure through interparticle interactions, both for static and deforming interfaces. Indeed, due to the Brownian motion of nanoparticles, the interparticle forces might still lead to the generation of surface pressure and the reduction in the apparent interfacial tension [24]. Note that nanoparticles at the fluid–fluid interface do not change water molecule interactions at the interface, thus the interfacial tension at the microscopic scale still remains unchanged compared to the uncoated interface.

In contrast, our experimental results show that microparticles of silica at the static air–liquid interface remain in static state since Brownian motion does not occur and thus there is no unbalanced interparticle forces. Microparticles at static interfaces therefore generate no surface pressure and that no change in the surface tension is expected. Moreover, it was observed in our experiments that a monolayer of close-packed microparticles of silica was formed at the interface (shown in Fig. 3e), compared with the loose packing for nanoparticles [24]. For the static bubble coated by microparticles, the surface tension at both macroscopic scale and microscopic scale do not change, due to balanced interparticle forces at the interface, in agreement with the results from our modified sessile bubble method.

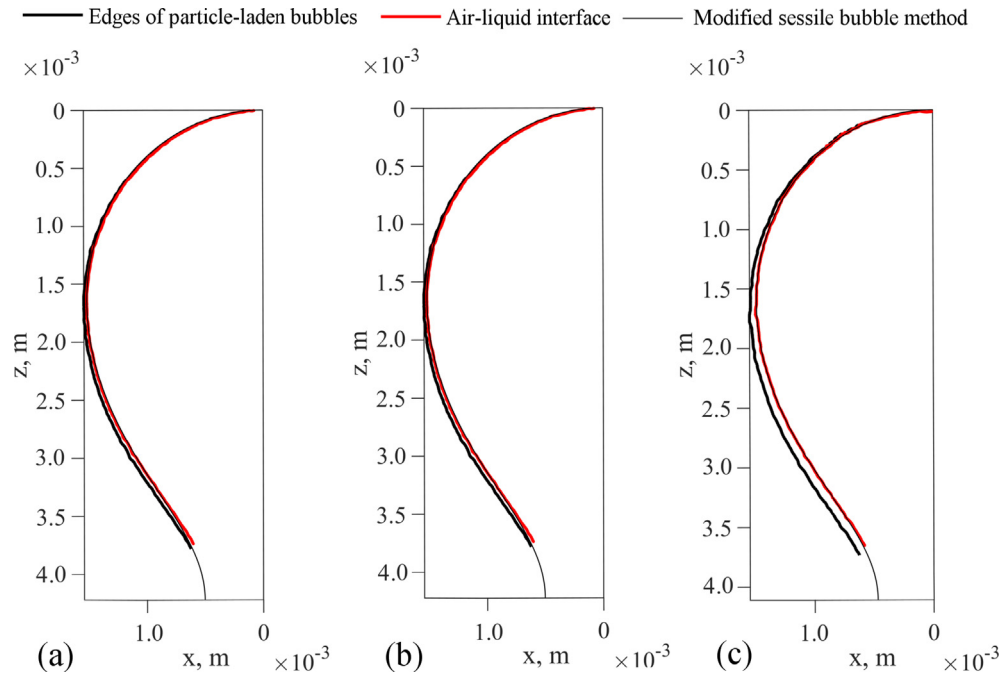

Fig. 7. Fittings obtained for particle-laden bubbles of three particle size classes: 27.5 μm (a), 45.5 μm (b) and 57.1 μm (c) using the modified sessile bubble method. The edges of particle-laden bubbles are shown as thick black lines. The air–liquid interface of the bubble, shown as red lines, were obtained by removing particles from the edges of particle-laden bubbles using erosion morphology during the image post-processing. Thin black lines are the fittings to the air–liquid interface of the bubble using the modified sessile bubble method.

Table 2
Surface tension (mN/m) obtained using the equations in the classical sessile bubble method and the modified method described in this work to fit the edges of particle-laden bubbles or the air–liquid interface.

Particle size (μm)	Classical sessile bubble method equations		Modified sessile bubble method equations	
	Particles not removed	Particles removed	Particles not removed	Particles removed
27.5	76.14	75.31	73.65	71.77
	75.48	74.23	73.20	72.36
	76.64	75.48	73.98	72.21
45.5	76.32	75.25	72.99	71.66
	78.83	76.07	73.17	71.98
	78.66	75.78	73.48	72.40
57.1	77.34	76.12	73.60	72.33
	75.91	75.28	73.19	72.15
	76.36	75.80	73.57	72.11

4.2. The effect of particle properties on the contour of a particle-laden bubble

To obtain a better understanding of why the classical sessile bubble method overestimates the surface tension of particle-laden bubbles, it is important to further analyse the role of particles in changing the bubble contour. To this end, the modified sessile bubble method is used in this section to investigate the contours of particle-laden bubbles of varying particle radius and contact angle. These contours are compared to those of uncoated bubbles.

According to Eqs. (1)–(4), the contour of uncoated bubbles can be predicted for a given surface tension, γ, density difference between the liquid and the air, $\Delta\rho$, and radius of curvature at the bubble apex, R. Fig. 8a shows the contour of three uncoated bubbles of different surface tension, as predicted by the classical sessile bubble method. The radius of curvature at the bubble apex was set to 1.28 mm and the density difference between the liquid and the air was set to 998 kg/m^3 for consistency in the comparisons for all cases in Fig. 8. The value of the radius of curvature at the bubble apex 1.28 mm was chosen to be slightly smaller than the experimental value of 1.41 mm in Section 4.1.1. Fig. 8a illustrates that the shape of the bubble becomes more slender as the surface tension decreases. This is because the buoyancy force stretches the bubbles while the surface tension opposes this trend by minimizing surface area. The decrease in the surface tension increases Bond number, meaning the importance of gravity over surface tension increases. The modified sessile bubble method was then used to analyse the shape of particle-laden bubbles for a case in which the surface tension of the bubbles, particle radius, particle density and particle contact angle were 60 mN/m, 150 μm, 40° and 2.5 g/cm^3, respectively. As it can be seen in Fig. 8b, the effect of particles attached to the bubble is similar to that of increasing the surface tension for uncoated bubbles; particles deform the bubble and make it more spherical. However, the mechanism behind the deformation of the bubble by particles differs from that of the uncoated bubbles since the microparticles at the air–liquid interface do not change the surface tension. The change in the contour of the particle-laden bubbles results from the interaction between the particles and the air–liquid interface through the pressure term P_{surf} in Eq. (6), which depends on particle contact angle, size, density and packing structure at the

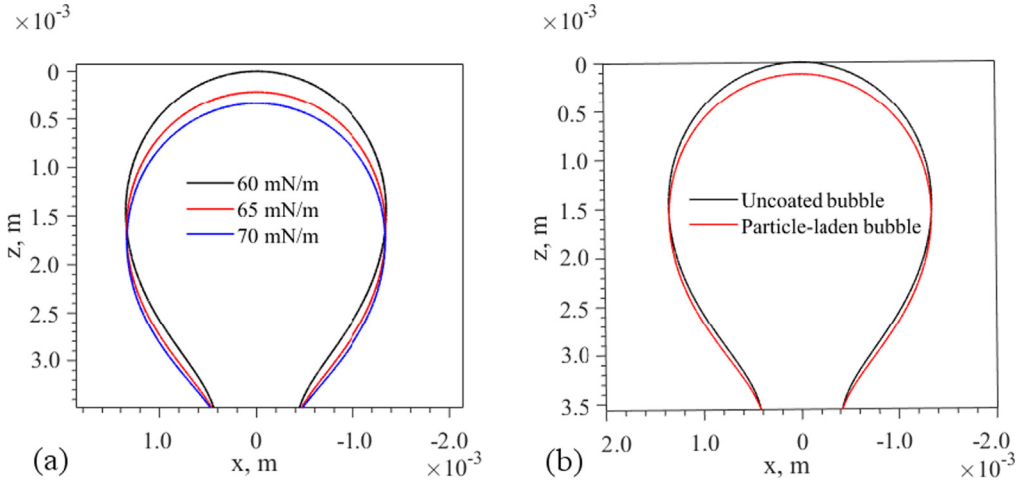

Fig. 8. (a) The contour of bubbles of different surface tension predicted using the classical sessile bubble method. (b) The comparison between the contour of an uncoated bubble and one coated with particles, where the prediction of the particle-laden bubble case was based on the modified sessile bubble method. The radius of curvature at the bubble apex was set to 1.28 mm. The surface tension of the bubbles was set to 60 mN/m in (b).

air–liquid interface as shown in Eq. (5). If the pressure term is not considered, i.e. if the surface tension of particle-laden bubbles is determined from Eqs. (1)–(4), the value tends to be larger than the real surface tension. The fact that particles have a similar effect on the bubble contour as that of the increase in interfacial surface tension explains why classical sessile bubble tensiometry (Table 1) yields larger surface tension values than those for uncoated bubbles despite particles not modifying the surface tension.

Fig. 9 shows the contour of the particle-laden bubbles of different particle properties investigated using the modified sessile bubble method, where the surface tension and radius of curvature at the bubble apex were set to 60 mN/m and 1.28 mm for comparison purposes. Regardless of the changes in particle properties, the contours of particle-laden bubbles all shift towards being more spherical compared to that of an uncoated bubble. The change in particle properties changes the particle forces exerted on the interfaces per unit area according to Eq. (5). Fig. 9a shows that increasing particle radius while keeping other particle properties fixed (i.e. contact angle 40°, particle density 2.5 g/cm^3 and hexagon packing at the bubble surface) shifts the bubble contour towards being more spherical as a result of the increase in the force between the particles and the interface. Similarly, the increase in the particle contact angle, while setting the particle radius as 50 μm and the packing structure to be hexagon packing, increases the force particles exert on the interfaces, resulting in a more spherical shape as shown in Fig. 9b. As the contact angle of the particles varies, the buoyancy force exerted on the particles changes since the proportion of particles in contact with the liquid changes. The change in buoyancy force for the particles leads to the change in the force between particles and the interface according to Eq. (5).

Microparticles of silica at the air–liquid interface of the bubbles are in static equilibrium, if bubbles do not experience dynamic processes such as oscillation [31], pinch-off [4] and coalescence [3,36]. By varying the particle properties, the force between the particles and the air–liquid interface changes, which leads to the change in the shape of the particle-laden bubbles. However, this does not imply that the particles change the surface tension of the particle-laden bubbles. The surface tension of the static particle-laden bubbles at microscopic scale is still the same as that of the uncoated bubbles, as confirmed using the modified sessile bubble method in section 4.1.2, since particles are in static equilibrium and no surface pressure is generated.

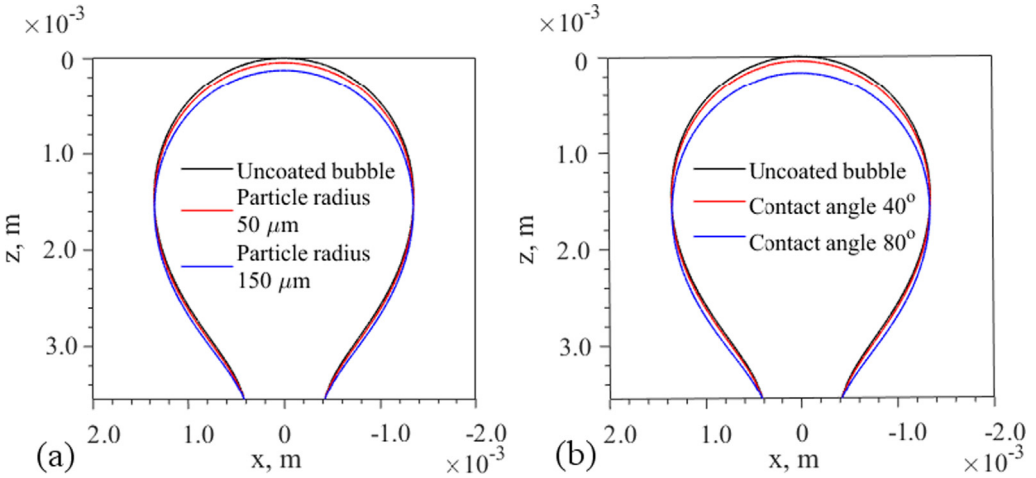

Fig. 9. The contour of the particle-laden bubbles with different particle sizes (a) and contact angles (b), predicted using the modified sessile bubble method. The surface tension was set to 60 mN/m in all cases. Particle radius was set to 50 μm in (b) for comparison purposes.

5. Conclusions

A modified sessile bubble method was developed to gain a fundamental understanding of the role of microparticles on the shape and surface tension of static particle-laden bubbles. Our method takes into account the force between the microparticles and the air–liquid interface, as opposed to the classical pendant drop method for uncoated interfaces [7] and nanoparticle-laden interfaces [24].

The image analysis technique presented in this work allows to obtain the contour of the air–liquid interface for microparticle-laden bubbles. By solving the partial differential equations derived for the modified sessile bubble method, the surface tension of static particle-laden bubbles with three different particle size classes were determined. The results show that the modified method correctly predicts the surface tension regardless of the presence of microparticles. Microparticles do not change the surface tension of the static particle-laden bubbles since particles are in static equilibrium and therefore no surface pressure is generated by interparticle forces. This differs from what occurs in nanoparticle-laden interfaces [20,26–28]. In contrast, the classical sessile bubble method is shown to overestimate the surface tension of microparticle-laden bubbles. It is relevant to note that the modified sessile bubble method developed in this work applies to monodispersed particles and that when considering polydispersed particles, Eq. (5) needs to be modified to consider different particle packing at the air–liquid interface. This was outside the scope of this work but warrants further investigation.

In addition, the modified sessile bubble method was used to investigate the contour of bubbles coated by particles with different contact angles and of different size. Interestingly, the results indicate that the monolayer of particles at the interface leads to a change in the bubble contour, similar to that caused by changes in surface tension for uncoated bubbles, which explains why classical sessile bubble tensiometry overestimates the surface tension of particle-laden bubbles.

The results from this work are important to understand the effect of microparticles on the shape and surface tension of static air–liquid interfaces. The modified sessile bubble method presented would make it possible to investigate the effect that the transfer of surfactant between particles and the air–liquid interface has on the surface tension of static particle-laden bubbles [36,38].

CRediT authorship contribution statement

H. Wang: Conceptualization, Data curation, Formal analysis, Investigation, Methodology, Validation, Visualization, Writing - original draft. **P.R. Brito-Parada:** Conceptualization, Investigation, Methodology, Supervision, Validation, Writing - review & editing, Funding acquisition.

Declaration of Competing Interest

The authors declare that they have no known competing financial interests or personal relationships that could have appeared to influence the work reported in this paper.

Acknowledgments

The authors would like to thank Peipei Wang and Francisco Reyes for the MATLAB routine for the classical sessile bubble method used in this work. H. Wang would like to thank the China Scholarship Council and Imperial College Joint Scholarship for financial support. P. Brito-Parada acknowledges funding from the European Union's Horizon 2020 research and innovation programme FineFuture under grant agreement No. 821265.

Appendix A. Supplementary material

Supplementary data associated with this article can be found, in the online version, at https://doi.org/10.1016/j.jcis.2020.11.094.

References

[1] B.P. Binks, T.S. Horozov, Aqueous foams stabilized solely by silica nanoparticles, Angew. Chem.-Int. Edit. 44 (2005) 3788–3791.
[2] T.S. Horozov, B.P. Binks, Particle-stabilized emulsions: A bilayer or a bridging monolayer?, Angew. Chem.-Int. Edit. 45 (2006) 773–776.
[3] H. Wang, P.R. Brito-Parada, Coalescence dynamics of particle-laden bubbles, Langmuir 36 (2020) 5394–5399.
[4] H. Wang, P.R. Brito-Parada, The pinch-off dynamics of bubbles coated by microparticles, J. Colloid Interface Sci. 577 (2020) 337–344.
[5] B. Petkova, S. Tcholakova, M. Chenkova, K. Golemanov, N. Denkov, D. Thorley, S. Stoyanov, Foamability of aqueous solutions: Role of surfactant type and concentration, Adv. Colloid Interface Sci. 276 (2020) 102084.
[6] M. Molaei, J.C. Crocker, Interfacial microrheology and tensiometry in a miniature, 3-d printed Langmuir trough, J. Colloid Interface Sci. 560 (2020) 407–415.
[7] J.D. Berry, M.J. Neeson, R.R. Dagastine, D.Y. Chan, R.F. Tabor, Measurement of surface and interfacial tension using pendant drop tensiometry, J. Colloid Interface Sci. 454 (2015) 226–237.
[8] K.D. Danov, R.D. Stanimirova, P.A. Kralchevsky, K.G. Marinova, N.A. Alexandrov, S.D. Stoyanov, T.B.J. Blijdenstein, E.G. Pelan, Method for determining the surface tension of drops and bubbles with isotropic and anisotropic surface stress distributions, J. Colloid Interface Sci. 440 (2015) 168–178.
[9] O. Ozdemir, S.I. Karakashev, A.V. Nguyen, J.D. Miller, Adsorption and surface tension analysis of concentrated alkali halide brine solutions, Miner. Eng. 22 (2009) 263–271.
[10] J.C. Burton, R. Waldrep, P. Taborek, Scaling and instabilities in bubble pinch-Off, Phys. Rev. Lett. 94 (2005) 184502.
[11] M.K. Tripathi, K.C. Sahu, R. Govindarajan, Dynamics of an initially spherical bubble rising in quiescent liquid, Nat. Commun. 6 (2015) 6268.
[12] B. Lalanne, O. Masbernat, F. Risso, Determination of interfacial concentration of a contaminated droplet from shape oscillation damping, Phys. Rev. Lett. 124 (2020) 194501.
[13] J.D. Paulsen, R. Carmigniani, A. Kannan, J.C. Burton, S.R. Nagel, Coalescence of bubbles and drops in an outer fluid, Nat. Commun. 5 (2014) 3182.
[14] D. Mesa, P.R. Brito-Parada, Scale-up in froth flotation: A state-of-the-art review, Sep. Purif. Technol. 210 (2019) 950–962.
[15] I. Mackay, A.R. Videla, P.R. Brito-Parada, The link between particle size and froth stability - Implications for reprocessing of flotation tailings, J. Clean. Prod. 242 (2020) 118436.
[16] A. Norori-McCormac, P.R. Brito-Parada, K. Hadler, K. Cole, J.J. Cilliers, The effect of particle size distribution on froth stability in flotation, Sep. Purif. Technol. 184 (2017) 240–247.
[17] E.M. Herzig, K.A. White, A.B. Schofield, W.C.K. Poon, P.S. Clegg, Bicontinuous emulsions stabilized solely by colloidal particles, Nat. Mater. 6 (2007).
[18] A. Jamburidze, A. Huerre, D. Baresch, V. Poulichet, M. De Corato, V. Garbin, Nanoparticle-coated microbubbles for combined ultrasound imaging and drug delivery, Langmuir 35 (2019) 10087–10096.
[19] S. Crossley, J. Faria, M. Shen, D.E. Resasco, Solid nanoparticles that catalyze biofuel upgrade reactions at the water/oil interface, Science 327 (2010) 68–72.
[20] V. Garbin, Collapse mechanisms and extreme deformation of particle-laden interfaces, Curr. Opin. Colloid Interface Sci. 39 (2019) 202–211.
[21] B.P. Binks, S.O. Lumsdon, Influence of particle wettability on the type and stability of surfactant-free emulsions, Langmuir 16 (2000) 8622–8631.
[22] C.G. Bell, C.J.W. Breward, P.D. Howell, J. Penfold, R.K. Thomas, A theoretical analysis of the surface tension profiles of strongly interacting polymer-surfactant systems, J. Colloid Interface Sci. 350 (2010) 486–493.
[23] R.I. Slavchov, J.K. Novev, Surface tension of concentrated electrolyte solutions, J. Colloid Interface Sci. 387 (2012) 234–243.
[24] V. Garbin, J.C. Crocker, K.J. Stebe, Forced desorption of nanoparticles from an oil-water interface, Langmuir 28 (2012) 1663–1667.
[25] V. Garbin, I. Jenkins, T. Sinno, J.C. Crocker, K.J. Stebe, Interactions and stress relaxation in monolayers of soft nanoparticles at fluid-fluid interfaces, Phys. Rev. Lett. 114 (2015) 108301.
[26] K. Casson, D. Johnson, Surface-tension-driven flow due to the adsorption and desorption of colloidal particles, J. Colloid Interface Sci. 242 (2001) 279–283.
[27] T. Li, K. Lilja, R.J. Morris, G.B. Brandani, Langmuir–blodgett technique for anisotropic colloids: Young investigator perspective, J. Colloid Interface Sci. 540 (2019) 420–438.
[28] T. Okubo, Surface tension of structured colloidal suspensions of polystyrene and silica spheres at the air-water interface, J. Colloid Interface Sci. 171 (1995) 55–62.

[29] A. Huerre, M. De Corato, V. Garbin, Dynamic capillary assembly of colloids at interfaces with 10,000g accelerations, Nat. Commun. 9 (2018) 3620.
[30] K. Hadler, J.J. Cilliers, The effect of particles on surface tension and flotation froth stability, Min. Metall. Explor. 36 (2018) 63–69.
[31] P. Wang, J.J. Cilliers, S.J. Neethling, P.R. Brito-Parada, The behavior of rising bubbles covered by particles, Chem. Eng. J. 365 (2019) 111–120.
[32] B.P. Binks, Particles as surfactants–similarities and differences, Curr. Opin. Colloid Interface Sci. 7 (2002) 21–41.
[33] Ş.S. Bayın, Ş.S. Bayin, Mathematical methods in science and engineering, Wiley Online Library, 2006.
[34] P. Wang, F. Reyes, J.J. Cilliers, P.R. Brito-Parada, Evaluation of collector performance at the bubble-particle scale, Miner. Eng. 147 (2020) 106140.
[35] J. Mingins, A. Scheludko, Attachment of spherical particles to the surface of a pendant drop and the tension of the wetting perimeter, J. Chem. Soc., Faraday Trans. 75 (1979) 1–6.
[36] S. Ata, Coalescence of bubbles covered by particles, Langmuir 24 (2008) 6085–6091.
[37] S. Ata, The detachment of particles from coalescing bubble pairs, J. Colloid Interface Sci. 338 (2009) 558–565.
[38] G. Bournival, S. Ata, E.J. Wanless, The roles of particles in multiphase processes: Particles on bubble surfaces, Adv. Colloid Interface Sci. 225 (2015) 114–133.
[39] U.T. Gonzenbach, A.R. Studart, E. Tervoort, L.J. Gauckler, Ultrastable particle-stabilized foams, Angew. Chem.-Int. Edit. 45 (2006) 3526–3530.